Materials and Manufacturing Processes

ISSN: (Print) (Online) Journal homepage: https://www.tandfonline.com/loi/lmmp20

Effect of grooving textured tool on the titanium chip morphology

Mehdi Gerami, Masoud Farahnakian & Sadegh Elhami Joosheghan

To cite this article: Mehdi Gerami, Masoud Farahnakian & Sadegh Elhami Joosheghan (2022) Effect of grooving textured tool on the titanium chip morphology, Materials and Manufacturing Processes, 37:9, 1013-1021, DOI: 10.1080/10426914.2021.2001515

To link to this article: https://doi.org/10.1080/10426914.2021.2001515

Published online: 30 Nov 2021.

MATERIALS AND MANUFACTURING PROCESSES
2022, VOL. 37, NO. 9, 1013–1021
https://doi.org/10.1080/10426914.2021.2001515

Taylor & Francis
Taylor & Francis Group

Effect of grooving textured tool on the titanium chip morphology

Mehdi Gerami[a], Masoud Farahnakian[a], and Sadegh Elhami Joosheghan[b]

[a]Mechanical Engineering Department, Najafabad Branch, Islamic Azad University, Najafabad, Iran; [b]Mechanical Engineering Department, Faculty of Engineering, Ferdowsi University of Mashhad, Mashhad, Iran

ABSTRACT

The observation of segmented chips in titanium alloy machining is a common phenomenon that leads to undesirable effects on tool life and characteristics of the machined surface. During grooving operation in the turning process, the contact area of the tool and workpiece is high, and the cross-section of the tool shank is small, which signifies the necessity of machinability improvement. The texture patterns have been recently used, which reduced the friction (force) and temperature of pair surfaces. Hence, in this study, linear and hole texture designs are considered on the rake face to investigate the effect of tool surface texture on chip morphology of TiAl6V4 titanium alloy during the grooving operations. The results showed that using texture on the tool's rake face at a 94 m/min cutting speed reduced the cutting force up to 38% compared to the simple tool. Also, the use of texture on the tool's rake face reduced the thickness of the chip up to 20% compared to the simple tool. Also, the linear texture design resulted in the lowest value of G and the highest value of fc, which means the most dynamic stability of the machining condition.

ARTICLE HISTORY
Received 30 August 2021
Accepted 7 October 2021

KEYWORDS
Texture; force; grooving; friction; morphology; segmentation; thickness; titanium

Introduction

Titanium alloys apply for particular purposes such as medical and aerospace due to their corrosion resistance and high hardness. However, the machinability of the titanium is low due to the small heat transfer coefficient, high modulus of elasticity, significant hardness at high temperatures, and chemical activity.[1–4]

In the production of some industrial parts, it is necessary to fabricate grooves on the internal or external surfaces of the workpiece. Grooving tools have a relatively narrow cutting edge, and to avoid contact of their sidewalls to the slotting walls of the workpiece, the side face of the tool is inclined inward and found a thin tool shank. Because the grooving tools are more delicate and have weaker support than the other, lower cutting forces and feed rates should be applied to prevent them from fracture and breaking. Hence, when the tool engages with and enters the workpiece, lubricant does not access the machining zone due to limited space, resulting in higher friction and cutting temperature and consequently reduces tool life. A solution should consider facilitating this problem.

Chip morphology plays a vital role in the cutting of metals. Segmented chips lead to undesirable effects on the tool life and characteristics of the machined surface. The mechanism of chip segmentation has not been found, yet but two mechanisms are presented in investigations. The first mechanism involves adiabatic shear due to the low heat transfer of titanium,[5,6] and the second considers the nucleation and growth of cracks.[7,8] Segmented chip is the origin of cyclic cutting forces. Characteristics of cyclic force are a function of segmentation specifications.[9,10]

The dynamics of the machining process originate from the mechanism of chip formation and plays an essential role in the tool life and wear.[11–13] The use of texture on cutting tools is an effective method that can modify the chip morphology. The use of texture on the cutting insert acts as a chip breaker and reduces the contact length of the chip and tool.[14] Also, texture leads to increasing the shear angle, which makes the chips shorter and finally provides more stability of the cutting process. Friction at the contact surface of the chip and rake face is a significant and influential factor in chip morphology[15] which can be influenced by surface texture.

Several strategies have been successfully used in the development of titanium alloys machining. The technique of using textures has recently become interesting with the development of micro/nano machining technologies. The friction reduction strongly depends on the shape and geometry of the texture. Significant friction reduction can be achieved using a micro or nano texture scale, which means improving the tribological properties at the contact surface of the tool and chip.[16,17] Several new technologies have been used to fabricate texture on contact surfaces and control the tribological properties, generally classified into mechanical methods, ion beam, etching, and energy beam techniques.

Thomas et al. studied the changes in cutting forces and their proportionality to chip formation mechanisms. In this study, various parameters such as cutting speed were investigated. Finally, it was found that the intermittent (cyclic) cutting force in the segmented state is 18% higher than in the case of the continuous chip.[18]

According to the theoretical analysis and numerical simulation, Bajpai et al. determined the critical speed at which chip segmentation is initiated. In terms of material properties,

CONTACT Masoud Farahnakian Farahnakian@gmail.com Mechanical Engineering Department, Najafabad Branch, Islamic Azad University, Najafabad, Iran

mentioned analysis and simulation depending on the chip thickness and tool angles. This procedure could provide reasonable predictions of the critical cutting speed to form a segmented chip.[19] Chip segmentation makes because of low local heat exchange associated with the α-β phase conversion at very high machining speeds. The current material models used in simulations of the machining process ignore the role of phase evolution in cutting and its effect on the material-related dynamic response. Hussain et al. developed a new approach by considering the mentioned subject to simulate the chip segmentation.[20]

Sivaiah et al. studied tools prepared with micro/nano textures for cutting the S35C steel to improve tool wear characteristics. The results showed that the linear texture with a depth of 150–100 nm and distance of 700 nm did not improve wear resistance. On the other hand, linear texture with a depth of 5 μm, a width of 20 μm, and a distance of 20 μm in a state parallel to the main cutting edge of a TiAlN coated tool significantly improved wear resistance and lubrication on the tool face.[21]

Sivaiah et al. performed experiments to determine the relation of the micro-textured tool and cutting forces. The results of orthogonal cutting experiments of 1045 steel showed that tool texture led to a reduction of cutting forces and friction coefficient at relatively high cutting speeds. The ratio of texture area to the total surface area was an effective parameter on the friction. Accurate examination of simple and textured tool and chip shapes showed that the changes in the shape and size of the chips effectively reduced cutting forces.[22]

Khani et al. employed textured tools during the thread turning process. They performed an experimental study to optimize the geometrical characteristics of the texture, such as depth, distance, and so on. They achieved more efficiency using hole texture in comparison to the linear design of texture.[23] In two other investigations, Khani et al. fabricated hole textures on the thread turning tools and filled them with MoS_2 solid lubricant. Mentioned tool led to reduction of cutting force components, built-up edge, and contact area during thread turning. They performed an experimental study and determined the optimized geometrical characteristics of the hole texture, such as hole diameter and distance.[24,25]

Previous researchers have not to pay attention to the employment of textured tools during grooving operation in the turning process and the effect of texture and cutting parameters on the chip shape and size. This research study the mentioned subjects during the grooving of Ti-6Al-4 V titanium alloy. Results are analyzed to determine the effect of cutting speed and texture designs on the cutting forces, chip shape, and size.

During the cutting of special materials such as titanium, there is a specific and critical cutting speed (V_c) which is the start point of chip segmentation.[26] The strain rate hardening phenomenon at lower speeds (V<Vc) leads to higher flow stress in the shear zone than in surrounding areas. In this condition, a continuous chip is expected to generate. At higher cutting speeds ($V>V_c$), flow stress does not increase the proportion to the cutting speed; hence thermoplastic instability is expected to happen during chip formation. Thermoplastic instability causes the shear phenomenon that occurs inside the shear plane in a manner that a segmented chip is generated. In this way, the following relation is expressed in determining the critical cutting speed:[26]

$$\begin{cases} \frac{d\tau}{dV}=0 \\ \tau=(\varepsilon_s,\dot{\varepsilon}_s,T) \end{cases} \Rightarrow \frac{d\tau}{dV}=\left.\frac{\partial\tau}{\partial\varepsilon_s}\right|_{(\dot{\varepsilon}_s,T)}\cdot\frac{d\varepsilon_s}{dV}+\left.\frac{\partial\tau}{\partial\dot{\varepsilon}_s}\right|_{(\varepsilon_s,T)}\cdot\frac{d\dot{\varepsilon}_s}{dV}+\left.\frac{\partial\tau}{\partial T}\right|_{(\varepsilon_s,\dot{\varepsilon}_s)}\cdot\frac{dT}{dV}=0 \tag{1}$$

in which flow stress (τ) can be defined as a function of shear strain (ε_s), shear strain rate ($\dot{\varepsilon}_s$) and temperature (T). The shear strain and shear strain rate can be stated as follows:

$$\begin{aligned} \varepsilon_s &= \frac{\cos(\gamma_0)}{\sin(\varphi)\cos(\varphi-\gamma_0)} \\ \dot{\varepsilon}_s &= \frac{\varepsilon_s V\sin(\varphi)}{s}=\frac{V\cos(\gamma_0)}{s\cos(\varphi-\gamma_0)} \end{aligned} \tag{2}$$

in which s is the thickness of the shear zone (Fig. 1). In Eq. (2), there is an essential parameter of φ, which is the angle of the shear plane (shear angle) (Fig. 1). φ can be evaluated according to the rake angle (γ_0), and cutting ratio (r) as follows:

$$\varphi=\operatorname{atan}\frac{r\cos\gamma_0}{1-r\sin\gamma_0},r=\frac{a_c}{a} \tag{3}$$

During the cutting process, three zones affect heat generation. Between them, the primary shear zone significantly affects the chip morphology, and study on its temperature can help identify the chip separation behavior. In the primary shear zone, the temperature can be evaluated as follows:

$$T=\frac{0.9\mu\tau\varepsilon_s}{\rho c}+T_0 \tag{4}$$

in which μ is the heat distribution coefficient. A more significant heat distribution coefficient is expected when higher values of cutting speed are applied because of the shorter available time for heat dissipation.

At the beginning of the process, the tool pushes the material at low cutting speeds, and plastic deformation occurs in the shear zone. Due to plastic deformation, heat is generated on the shear plane, and the temperature rises in the cutting zone. The continuous movement of the tool causes the increase of pushing force (overcoming the friction of the rake face) that pushes the deformed material on the rake face. The movement of the chip prevents further deformation in the shear zone, and this process continues, and a continuous chip is created with a very small saw-tooth on the free surface of the chip.

During the implementation of higher cutting speeds, the shear zone temperature rises rapidly because of the more adiabatic thermal conductivity, leading to lower values of material flow stress. The continuous movement of the tool and increase of pushing force due to low flow stress of the material does not overcome the frictional force of the rake face. So more material is deformed in the shear zone, and material accumulates and compresses until the pushing force can overcome the friction force. Therefore, after a pause in the movement of the chip, a slip will occur and cause the segmented chip. Thus, for the higher values of the cutting speed, the shear zone temperature increases and causes more thermal softening of the material, which causes the rise of segmentation.

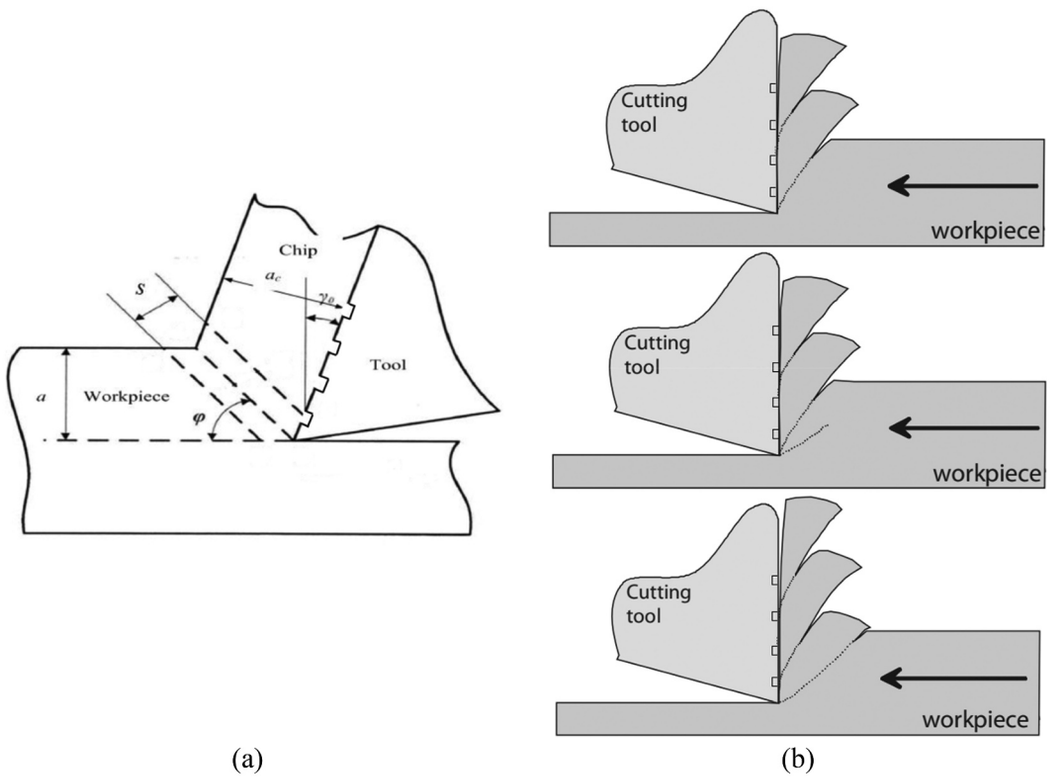

Figure 1. (a) Orthogonal model of cutting (b) Steps of chip segmentation.

Materials and methods

A TN50D lathe Machine performed the experiments. The workpiece included a TiAl6V4 titanium shaft with a diameter of 30 mm and a length of 45 cm (Fig. 2a). The tool holder of the lathe was equipped with a 9255B Kistler dynamometer to measure cutting forces in three directions (Fig. 2b). Some initial disks were made on the workpiece to prevent the chip removal by the side cutting edge (Fig. 2a). Every disk was used for an individual experiment. Mentioned condition provided the orthogonal cutting with a cutting width of 3.5 mm.

The tool was a Tungsten Carbide grooving tool with a width of 3.5 mm and a clearance angle of 16°, a side angle of 3°, and without rake angle in which rake face was modified by a femtosecond laser to fabricate textures.

The texture is considered with two designs of the hole and linear pattern (Fig. 3a). Considering the specification of a femtosecond laser, the depth of texture was about 13 μm (Fig. 3b). After the experiments, the chips were collected and prepared for metallography (etching) and imaging using a light microscope. Etching was done by Kroll's solution and etching time of 30 s.

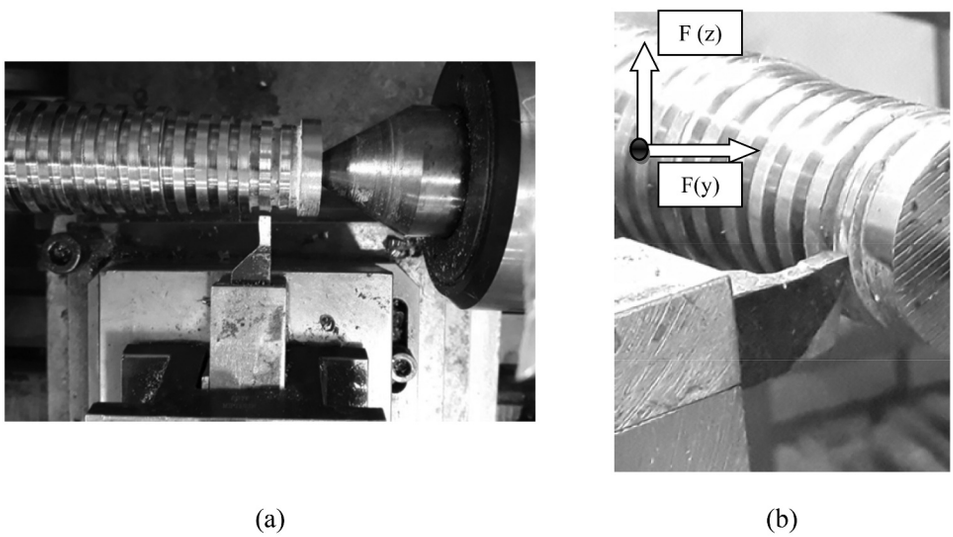

Figure 2. (a) Workpiece (b) Directions of force components.

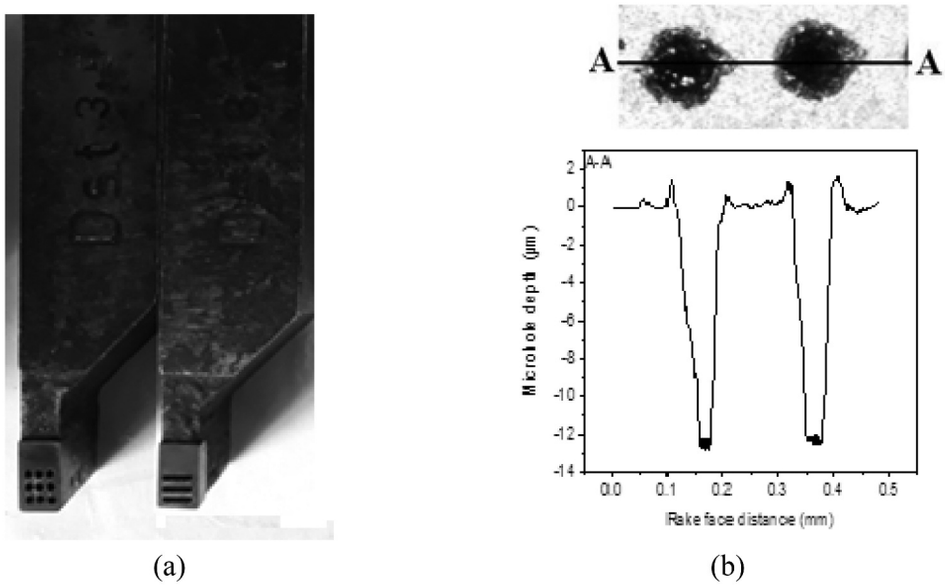

Figure 3. (a) Hole and linear texture designs (b) Depth of the (hole) texture.

Table 1. Parameters and levels of experiments.

Parameter	Levels				
Cutting speed (m/min)	*17*	*24*	*48*	*67*	*94*
Texture pattern	*Simple (without texture)*		*Hole design*	*Linear design*	

The feed was considered constant equal to 0.4 mm/rev, and each experiment was repeated three times to ensure the accuracy of the results. The experimental design is presented in the following Table 1:

Results and discussion

According to Fig. 4, two force components of F(z) (perpendicular to the tool rake face) and F(y) (perpendicular to the tool flank face) at five levels of cutting speed and two states of texture are compared. Generally, it can be seen that both texture designs present the reduction of force components related to the simple tool.

It is observed that increasing the cutting speed for the textured tool F(y) graph presents a smoother reduction slope compared to the force components of F(z). The most significant reduction in cutting force is observed in the tool with a linear pattern parallel to the cutting edge. Reducing the contact area of the chip and tool rake face minimizes the friction and consequently decreases the cutting force components for textured tools compared to simple tools. A textured tool with a linear pattern parallel to the cutting edge led to a 16% to 38% reduction of force components which was higher than another texture pattern (hole). In general, different texture designs on the tool rake face had reduced the cutting forces by about 6% to 38% compared to the simple tool. Implementation of texture shrinks the area of contact; hence, lower friction force was expected while sliding two contact surfaces.

According to Fig. 5a, the segmented chip includes several teeth, which should be described quantitatively by the following parameters:

L: length of a tooth (pyramid) edge
h: chip thickness in the valley of a tooth
h_c: chip thickness in the peak of a tooth
P: distance of two consequent peaks (pitch)
φ: shear angle

According to Fig. 5b, it can be observed that the chip obtained from the textured tool at a cutting speed of 17 m/min presents a lower segmentation phenomenon compared to the simple tool. Segmentation phenomenon can be determined through the teeth specifications, especially parameters of h and h_c. In lower cutting speeds, h and h_c find relative values. Simultaneously, L and P reach the minimum possible values. Reverse values are expected at higher cutting speeds, as shown in Fig. 5b (V = 94 m/min). During the variation of the cutting speed from 47 to 94 m/min, a more segmented chip appears.

The mean thickness of the segmented chip can be defined as:

$$a_c = \frac{h + h_c}{2} \tag{5}$$

Figure 6 shows the mean chip thickness diagram for simple and two texture designs at five levels of cutting speed. According to the graph, cutting speed presents a direct relation to the chip thickness. For the textured tool, the diagram finds a slower increasing slope compared to the simple tool. Also, at a cutting speed of 94 m/min, the chip thickness of the simple tool found larger values about 0.15 to 0.3 mm compared to the textured tools. It means that for textured tools, the mean chip thickness was 10% to 20% smaller than a simple tool that is an important achievement according to the effect of chip

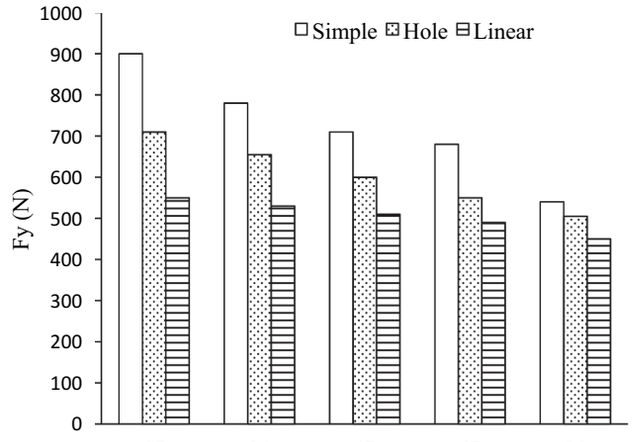

		Vc (m/min)	17	24	47	67	94
Reduction Percentage (%)	Hole design		21	16	15	19	6
	Linear design		38	32	28	27	16

(a)

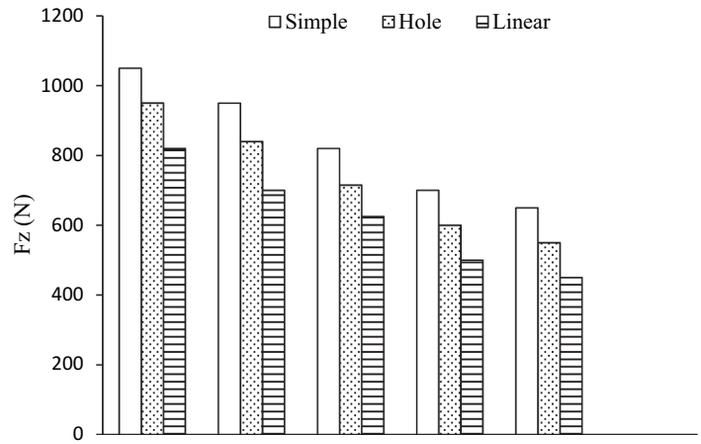

		Vc (m/min)	17	24	47	67	94
Reduction Percentage (%)	Hole design		9	12	13	14	15
	Linear design		22	26	23	29	31

(b)

Figure 4. The effect of texture on the cutting force components (a) F(y) (b) F(z).

thickness on the power consumption during the cutting process. Between texture designs, the linear pattern obtained smaller thickness values which is an exciting achievement.

Dynamic stability of the machining process is a function of variations of cutting force components. On the other hand, cutting forces are evaluated based on chip geometry; hence, machining stability can be analyzed through the changes in chip geometry. In this way, the geometry variation of the chip is studied by defining two parameters parallel and normal to the chip movement direction. Segmentation degree (G) is defined as normal to the chip movement direction by peak and valley thicknesses (h_c and h). Segmentation frequency is expressed parallel to the chip movement direction by cutting speed (V) and the tooth pitch (P).

The segmentation degree (G) can be calculated as follows:

$$G = \frac{h_c - h}{h_c} \tag{6}$$

In Fig. 7, the vertical axis shows the G parameter. Smaller values show the uniform chip thickness and higher values used for chips with large teeth (high degree of segmentation). According to Fig. 7, cutting speed presents a direct relation to the G parameter. According to the rising cutting speed, the shear zone temperature increases and causes more softening of the material. Hence, more compressed material is released, and a higher strain rate leads to the great movement of chip normal to the rake face which finally h_c finds a large value. Due to mass conservation and high-speed movement of the chip in the neighbor of the shear plane, h finds a lower value. The teeth of the segmented chip make a triangle shape in which P is related

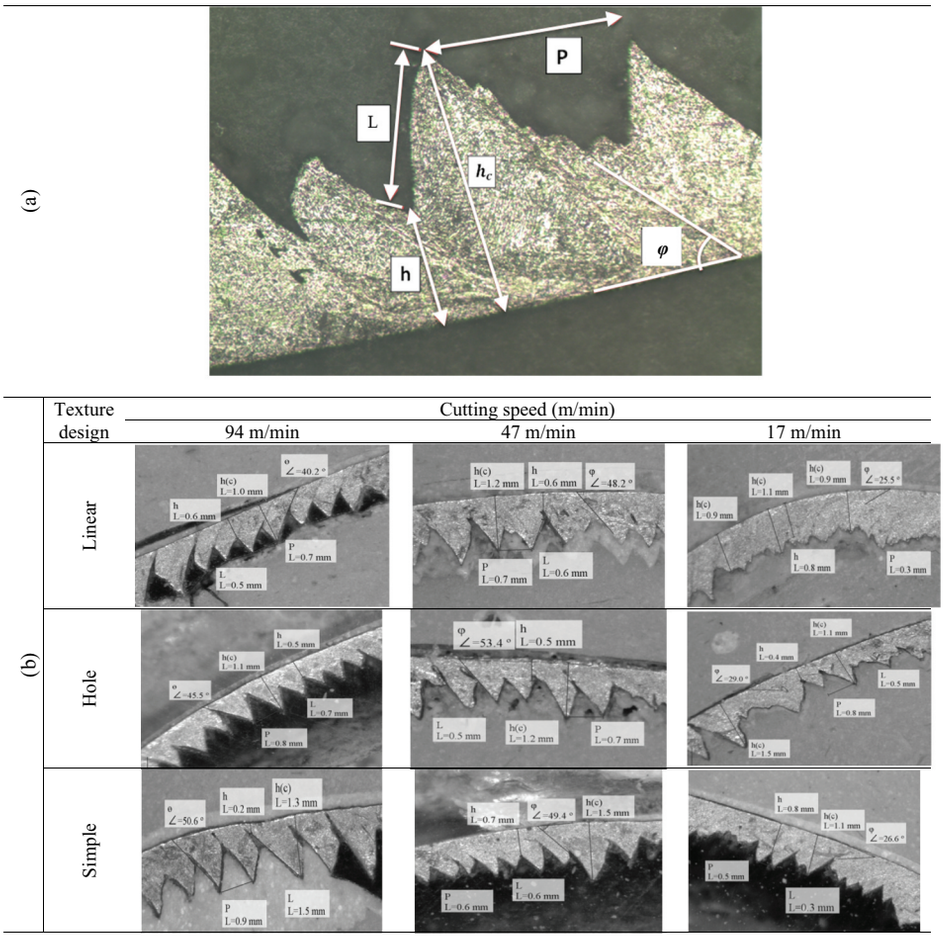

Figure 5. (a) Characteristics of a tooth in the segmented chip (b) Segmented chip characteristics for simple and textured tools.

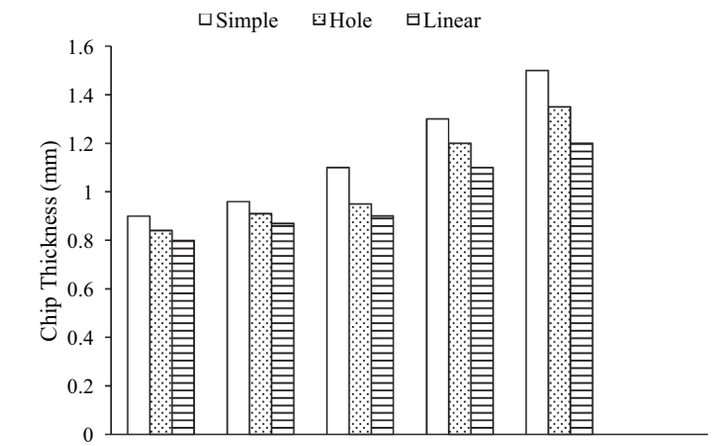

Reduction Percentage (%)						
	Hole design	7	5	14	8	10
	Linear design	11	9	18	15	20

Figure 6. The effect of cutting speed and texture design on the mean chip thickness.

to the difference of h and hc. Totally and considering the mentioned condition, a higher value of h_c and a smaller value of h results in a larger *P* value and greater chip segmentation.

A simple tool provided a higher growth of G parameter compared to the textured tool. Between textured tools, the linear design showed the smallest growth of the G parameter with a 48% G reduction percentage compared to the simple tool.

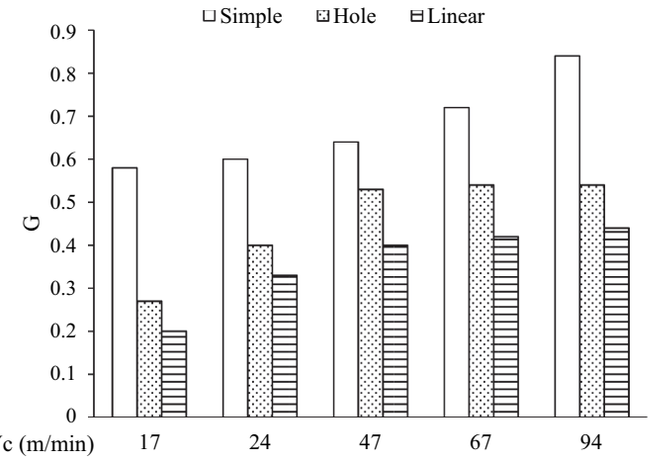

Vc (m/min)		17	24	47	67	94
Reduction Percentage (%)	Hole design	54	33	17	25	36
	Linear design	65	45	37	42	48

Figure 7. The effect of cutting speed and texture design on the segmentation degree (G).

Burns et al. assumed that Hook's Law could be employed to establish a relation between local compressive stress and strain. Compressive strain rate can be defined by the variation of speed in the direction of shear and the local velocity of workpiece material in a specific length. In this way, the variation rate of compressive stress can be stated according to the elastic modulus of the workpiece materials and compressive strain rate as follow..[27]

$$\frac{\partial \sigma}{\partial t} = \Lambda \frac{V_s - v}{\delta} \tag{7}$$

V_s in turning can be evaluated according to shear angle, rake angle, and cutting speed. Considering the material behavior in a large deformation as rigid-thermoviscoplastic, it can be concluded that elastic shear strain is negligible, and plastic strain rate equals to shear strain rate. In turning, v is known as the chip's speed, which moves on the rake face away from the tool. In this condition, the employment of texture reduced the resistive friction force and applied it on the chip. Hence, the chip speed in the direction of away from the tool increases. Also, according to Eq. (7), the variation rate of compressive stress reduces. It means that smaller chip segmentation is expected.

f_c shows the segmentation frequency, which can be evaluated as follows..

$$f_c = \frac{V}{P} \tag{8}$$

V is the cutting speed (mm/sec), and P is the tooth pitch (mm). f_c states the stability of the machining process. Increasing the cutting speed leads to higher values of f_c. For textured tools, f_c found larger values than the simple tool and increasing the cutting speed signified mentioned differences. The linear design of the texture achieved the highest values of f_c compared to the hole texture design (Fig. 8).

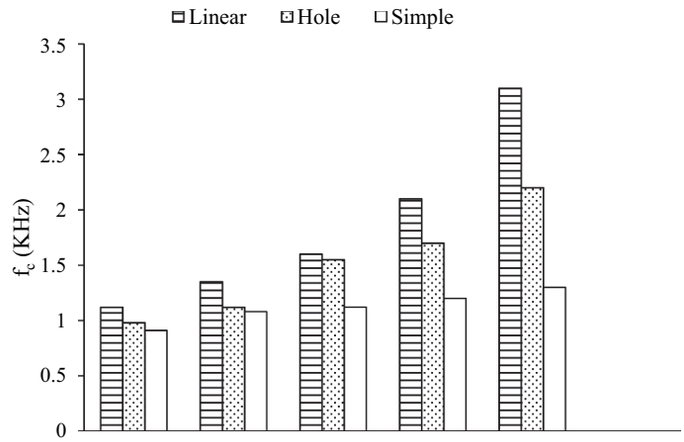

Vc (m/min)		17	24	47	67	94
Variation Percentage (%)	Hole design	8	4	38	41	69
	Linear design	23	25	43	75	138

Figure 8. The effect of cutting speed and texture design on the segmentation frequency.

Conclusions

This research studied the effect of rake face texture on the chip morphology during titanium machining. Generally, textured tools reduced the chip segmentation during titanium grooving operation in the turning process, resulting in lower cutting forces and a more stable machining process. Hence, according to industrials aspects, higher material removal can be applied during cutting, and a more efficient process is archived. Achieved results can be classified as follows:

- Reducing the contact area of the chip and tool rake face reduced the friction and, consequently, reduced the cutting force components using textured tools compared to simple tools. Textured tools with linear patterns parallel to the cutting edge led to a 16% to 38% reduction of force components.
- Cutting speed presented a direct relation to the chip thickness. Also, for textured tools, the mean chip thickness was 10% to 20% smaller than a simple tool.
- The degree of segmentation (G) presented a direct relation to the cutting speed. In higher cutting speed, significant growth of thermal softening and more strain rate was applied to the material and larger elastic energy stored in the material before the shear phenomenon. In the moment of the shear phenomenon, elastic energy was released, and besides higher strain rate led to the great movement of chip normal to the rake face that finally h_c found a large value.
- The simple tool achieved a higher increase rate of G according to cutting speed than the textured tool. Between textured tools, the linear design showed the smallest growth of the G parameter with a 48% G reduction percentage compared to the simple tool. The employment of texture caused the chip speed in the direction of away from the tool to increase and the variation rate of compressive stress reduced. It meant that smaller chip segmentation was expected.
- Increasing the cutting speed resulted in higher differences of f_c between simple and textured tools. The highest segmentation frequency was achieved for linear texture design, which stated the more stable machining process.

Disclosure statement

No potential conflict of interest was reported by the author(s).

References

[1] Elhami, S.; Razfar, M.; Farahnakian, M.; Rasti, A. Application of GONNS to Predict Constrained Optimum Surface Roughness in Face Milling of High-silicon Austenitic Stainless Steel. *Int. J. Adv. Manuf. Technol.* 2013, 66(5–8), 975–986. DOI: 10.1007/s00170-012-4382-y.

[2] Leo Kumar, S.; Avinash, D. Investigations on Achievable Surface Quality in Milling of Ti-35Nb-7Zr-5Ta Alloy. *Mater. Manuf. Processes* 2021, 36, 1800–1806. Published Online Jul 05. DOI: 10.1080/10426914.2021.1948054.

[3] Selvakumar, S.; Sreebalaji, V.; Ravikumar, K. Machinability Analysis and Optimization in Micro Turning on Tool Wear for Titanium Alloy. *Mater. Manuf. Processes*. 2021, 36(7), 792–802. DOI: 10.1080/10426914.2020.1866198.

[4] Elhami, S.; Razfar, M.; Farahnakian, M. Experimental Study of Surface Roughness and Tool Flank Wear during Hybrid Milling. *Mater. Manuf. Processes*. 2016, 31(7), 933–940. DOI: 10.1080/10426914.2015.1048474.

[5] Pervaiz, S.; Rashid, A.; Deiab, I.; Nicolescu, M. Influence of Tool Materials on Machinability of Titanium-and Nickel-based Alloys: A Review. *Mater. Manuf. Processes*. 2014, 29(3), 219–252. DOI: 10.1080/10426914.2014.880460.

[6] Xu, J.; Zhou, L.; Chen, M.; Ren, F. Experimental Study on Mechanical Drilling of Carbon/epoxy composite-Ti6Al4V Stacks. *Mater. Manuf. Processes*. 2019, 34(7), 715–725. DOI: 10.1080/10426914.2019.1594275.

[7] Vyas, A.; Shaw, M. Mechanics of Saw-tooth Chip Formation in Metal Cutting. *J. Manuf. Sci. Eng.* 1999, 121(2), 163–172. DOI: 10.1115/1.2831200.

[8] Mahesh, K.; Philip, J. T.; Joshi, S.; Kuriachen, B. Machinability of Inconel 718: A Critical Review on the Impact of Cutting Temperatures. *Mater. Manuf. Processes*. 2021, 36(7), 753–791. DOI: 10.1080/10426914.2020.1843671.

[9] Jaiswal, A. P.; Khanna, N.; Bajpai, V. Orthogonal Machining of Heat Treated Ti-10-2-3: FE and Experimental. *Mater. Manuf. Processes*. 2020, 35(16), 1822–1831. DOI: 10.1080/10426914.2020.1802039.

[10] Ming, W.; Dang, J.; An, Q.; Chen, M. Chip Formation and Hole Quality in Dry Drilling Additive Manufactured Ti6Al4V. *Mater. Manuf. Processes*. 2020, 35(1), 43–51. DOI: 10.1080/10426914.2019.1692353.

[11] Gowthaman, S.; Jagadeesha, T. Experimental Investigation on Friction Formation during Slot Milling of Nimonic263. *Mater. Manuf. Processes*. 2021, 36(12), 1403–1413. DOI: 10.1080/10426914.2021.1906899.

[12] Khajehzadeh, M.; Moradpour, J.; Razfar, M. R. Influence of Nanofluids Application on Contact Length during Hard Turning. *Mater. Manuf. Processes*. 2019, 34(1), 30–38. DOI: 10.1080/10426914.2018.1532091.

[13] Khajehzadeh, M.; Moradpour, J.; Razfar, M. R. Influence of Nanolubricant Particles' Size on Flank Wear in Hard Turning. *Mater. Manuf. Processes*. 2019, 34(5), 494–501. DOI: 10.1080/10426914.2019.1566619.

[14] Wang, X.; Jawahir, I. Prediction of Tool-chip Interface Friction and Chip-groove Effects in Machining with Restricted Contact Grooved Tools Using the Universal Slip-line Model. *Key Eng. Mater.* 2003, 233–236, 469–476. Trans Tech Publ. https://doi.org/10.4028/www.scientific.net/KEM.233-236.469 .

[15] Mikołajczyk, T.; Latos, H.; Pimenov, D. Y.; Paczkowski, T.; Gupta, M. K.; Krolczyk, G. Influence of the Main Cutting Edge Angle Value on Minimum Uncut Chip Thickness during Turning of C45 Steel. *J. Manuf. Processes*. 2020, 57, 354–362. DOI: 10.1016/j.jmapro.2020.06.040.

[16] Elias, J. V.; Venkatesh, N. P.; Lawrence, K. D.; Mathew, J. Tool Texturing for Micro-turning Applications–an Approach Using Mechanical Micro Indentation. *Mater. Manuf. Processes*. 2021, 36 (1), 84–93. DOI: 10.1080/10426914.2020.1813899.

[17] Sivaiah, P.; Revantha Kumar, M.; Bala Subramanyam, S.; Prasad, K. A Comparative Study on Different Textured and Untextured Tools Performance in Turning Process. *Mater. Manuf. Processes*. 2021, 36 (8), 926–935. DOI: 10.1080/10426914.2020.1866201.

[18] Jesudass Thomas, S.; Kalaichelvan, K. Comparative Study of the Effect of Surface Texturing on Cutting Tool in Dry Cutting. *Mater. Manuf. Processes*. 2018, 33(6), 683–694. DOI: 10.1080/10426914.2017.1376070.

[19] Bajpai, V.; Lee, I.; Park, H. W. Finite Element Modeling of Three-dimensional Milling Process of Ti–6Al–4V. *Mater. Manuf. Processes*. 2014, 29(5), 564–571. DOI: 10.1080/10426914.2014.892618.

[20] Hussain, M.; Siemers, C.; Rösler, J. Development of a Free-machining (α+ β) Titanium Alloy Based on Ti-6Al-2Sn-4Zr-6Mo. *Mater. Manuf. Processes*. 2013, 28(5), 545–549. DOI: 10.1080/10426914.2012.746781.

[21] Sivaiah, P.; Singh, M. M.; Venkatesu, S.; Yoganjaneyulu, G. Investigation on Turning Process Performance Using Hybrid-textured Tools under Dry and Conventional Cooling Environment. *Mater. Manuf. Processes*. 2020, 35(16), 1852–1859. DOI: 10.1080/10426914.2020.1813893.

[22] Sivaiah, P.; Guru Prasad, M.; Singh, M. M.; Uma, B. Machinability Evaluation during Machining of AISI 52100 Steel with Textured Tools under Minimum Quantity Lubrication–A Comparative Study. *Mater. Manuf. Processes*. 2020, 35(15), 1761–1768. DOI: 10.1080/10426914.2020.1802034.

[23] Khani, S.; Razfar, M. R.; Haghighi, S. S.; Farahnakian, M. Optimization of Microtextured Tools Parameters in Thread Turning Process of Aluminum 7075 Aerospace Alloy. *Mater. Manuf. Processes*. 2020, 35(12), 1330–1338. DOI: 10.1080/10426914.2020.1772485.

[24] Khani, S.; Haghighi, S. S.; Razfar, M. R.; Farahnakian, M. Optimization of Dimensional Accuracy in Threading Process Using Solid-lubricant Embedded Textured Tools. *Mater. Manuf. Processes* 2021, 1–11, Published Online May 14. DOI: 10.1080/10426914.2021.1926492.

[25] Khani, S.; Shahabi Haghighi, S.; Razfar, M. R.; Farahnakian, M. Improvement of Thread Turning Process Using Micro-hole Textured Solid-lubricant Embedded Tools. *Proc. Inst. Mech. Eng. Part B*. 2021, 235(11), 1727–1738. DOI: 10.1177/09544054211019929.

[26] He, L.; Su, H.; Xu, J.; Zhang, L. Study on Dynamic Chip Formation Mechanisms of Ti2AlNb Intermetallic Alloy. *Int. J. Adv. Manuf. Technol.* 2017, 92(9), 4415–4428. DOI: 10.1007/s00170-017-0527-3.

[27] Burns, T. J.; Davies, M. A. Nonlinear Dynamics Model for Chip Segmentation in Machining. *Phys. Rev. Lett.* 1997, 79(3), 447. DOI: 10.1103/physrevlett.79.447.